Amirkabir Journal of Mechanical Engineering

Amirkabir J. Mech. Eng., 53(11) (2022) 1345-1348
DOI: 10.22060/mej.2021.19257.6989

Effect of Magnetic Field on Motion, Deformation, and Separation Time of Newtonian and Non-Newtonian Droplets in a Flow-Focusing Microchannel

S. Mas-hafi, M. Esmaeili*

Department of Mechanical Engineering, Kharazmi University, Tehran, Iran

ABSTRACT: In the present study, the effect of external magnetic field on the process of droplet formation with different sizes and frequencies in a flow-focusing micro-channel is numerically studied. Moreover, the influence of non-Newtonian properties on the droplet formation characteristics is investigated using two non-Newtonian Carreau and power-law models. To solve the continuity and momentum equations for unsteady, two-phase, and incompressible flow, the finite volume method is employed. A numerical algorithm based on the volume-of-fluid technique is used to determine the effect of Bond number (0 to 0.2) and Power-law indices (0.3, 0.6, and 1.3) on the droplet formation process along with their size and separation time. To validate the numerical solution, the formation of Newtonian fluid droplets at different values of magnetic field strength is compared with the results of other studies and very good agreement was observed. The results of the numerical solution show that the Carreau fluid droplet in the Bond number of 0.2 has the highest volume, which is equivalent to the dimensionless volume of 1.56. Also, the process of droplet formation is more affected by the magnetic field than by the non-Newtonian model. Besides, with developing the field strength, droplet separation time increases and as a result, larger droplets with lower frequency will be formed.

Review History:

Received: Nov, 14, 2021
Revised: Feb. 27, 2021
Accepted: Feb. 28, 2021
Available Online: Mar. 11, 2021

Keywords:

Microfluidic
Droplet formation
Magnetic field
Non-Newtonian fluid
Numerical simulation.

1- Introduction

Microfluidic droplets are generated by the injection of immiscible fluids into the microchannel structures. Fluid manipulation such as droplet generation, mixing, sorting, and transport is accomplished in active and passive manners. Droplet size and production frequency can be controlled by adjusting flow rate, viscosity, and interfacial tension. Various active mechanisms have utilized external fields among which magnetic field is popular where magnetic particles inside a drop allow the precise control and manipulation of droplets. In general, passive and active microfluidic devices are applicable in the separation of biological particles such as blood and tumor cells. These devices provide improved sensitivity, efficiency, and operational range.

Experimental/numerical studies have investigated the effect of magnetic fields on droplets in different geometries. In a T-junction [1], an upstream magnet, pulls the ferrofluid droplets back, prolonging the production cycle and increasing the size of the droplets. The downstream magnet, however, acts oppositely. Investigation of the flow-focusing structure [2] concludes that droplet size depends highly on the flow rate, magnetism, magnetic field gradient, and location. The droplets' response also changes according to the viscosity described by different functions. These results explain the basis of droplet microfluidics, facilitating the applications. The numerical study of non-Newtonian droplet generation in a co-flowing structure reveals that in the jet regime, the volume of droplets is less dependent on the viscosity [3].

Recent studies explored the effect of magnetic field and viscosity. However, their simultaneous effect has not been studied in any flow-focusing device yet. Thus, in the present study, the flow-focusing channel was investigated for Newtonian and non-Newtonian fluids while changing the Bond number from 0 to 0.2. Two non-Newtonian viscosity models were used: Carreau and power-law. The velocity and pressure fields were compared during the analysis process as well as the droplet size and separation times. Also, for B_m=0.1, the droplet formation process was studied for power-law fluids of n = 0.3, n = 0.61 and n = 1.3.

2- Methodology

The droplet formation in a flow-focusing configuration was investigated with/without a magnetic field. The computational

$$\nabla \cdot (\vec{u}) = 0 \tag{1}$$

$$\frac{\partial}{\partial t}(\rho\vec{u}) + \nabla \cdot (\rho\vec{u}\vec{u}) = -\nabla p + \nabla \cdot \tau + \vec{F} \tag{2}$$

$$= -\nabla p + \nabla \cdot \tau - \sigma\kappa n_f D(\phi) - \frac{1}{2}\mu_0 \left|\vec{H}\right|^2 \nabla \chi_m$$

$$\tau = \eta_{eff}\left[\nabla\vec{u} + (\nabla\vec{u})^T\right] \tag{3}$$

*Corresponding author's email: m.esmaeili@khu.ac.ir

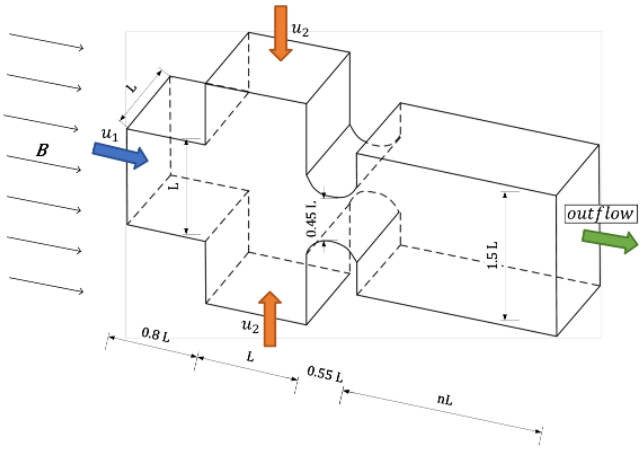

Fig. 1. Computational domain and the magnetic field setup. The channel width and height are L=100 µm.

domain illustrated in Fig. 1, consists of immiscible continuous and dispersed fluids entering the side and main-channel, respectively. The governing equations are the continuity and momentum in transient form while the non-Newtonian shear stress changes with the deformation tensor (Eqs. (1) to (3)).

Due to the symmetric flow and geometry, only 1/4 of the domain is calculated reducing the computations. The no-slip walls and outlet output boundary conditions were applied. Magnetic body force is defined on the interface as the last right-side phrase of Eq. (2) where μ_0 is the free space permeability constant, H the magnetic field strength, and χm the ferrofluid magnetic susceptibility. The susceptibility gradient, proportional to the phase gradient, results in the interface tracking via Eqs. (4) and (5). The dimensionless Bond number was used indicating the effect of the magnetic field along with the dimensionless numbers described in Eq. (6).

$$\nabla\chi_m = \frac{d\chi_m}{d\phi}\nabla\phi, \quad \frac{1}{1+\chi_m} = \frac{1-\phi}{1+\chi_{m^-}} + \frac{\phi}{1+\chi_{m^+}} \tag{4}$$

$$\frac{d\chi_m}{d\phi}\frac{(1+\chi_{m^+})(1+\chi_{m^-})(\chi_{m^+}-\chi_{m^-})D(\phi)}{\left[(1+\chi_{m^+})+H(\chi_{m^-}-\chi_{m^+})\right]^2} \tag{5}$$

$$B_m = \mu_0 LH^2/\sigma, \quad Ca = \mu_1\mu_2/\sigma, \quad \mathrm{Re} = \rho_2 u_2 L/\mu_2 \tag{6}$$

where $\mu 1$ is the dispersed phase viscosity and μ_2, ρ_2, u_2 define the continuous phase viscosity, density, and velocity, respectively. σ defines the interfacial tension of phases. The continuous phase is Newtonian, while Newtonian, non-Newtonian Carreau, and power models have been used for the dispersed phase viscosity models as:

$$\eta = \eta_\infty + \Delta\eta/(1+(\lambda\dot{\gamma})^m)^a \tag{7}$$

Table 1. Material properties and model assumptions with σ=13 mN/m, µc=2 mPa.s, ρc=1100, ρd=960 kg/m3, Qc=10 and Qd=5 µl/h.

	η [mPa.s]		B_m	$Re_d \times 10^4$	$Ca_d \times 10^4$
Dispersed phase (ferrofluid)	μ=96		0 0.1	76.4	0.023
	3.5+52.5/ (1+(3.313 $\dot{\gamma}$)^2)$^{0.3216}$		0 0.1 0.2	2.73	0.648
	0.42$\dot{\gamma}^{n-1}$	n=0.3	0.1	1.24	1.43
		n=0.61		1.802	2.20
		n=1.3		0.187	9.43

$$\eta = k\dot{\gamma}^{n-1} \tag{8}$$

where η∞ is the infinite-plane shear viscosity, Δη its difference with zero-plane viscosity. λ, a and k denote the time and power-law index (a=-(n-1)/2) and a measure of mean viscosity, respectively. Table 1 illustrates the fluid properties and other flow conditions applied. The dimensionless numbers for the present study for the continuous phase, Ca_c = 2.22 ×10-4, and Re_c = 2.78 ×10-4, are constant.

The 3D-Finite Volume (FV) method has been employed to solve the governing equations. In addition, fluid density was assumed to change linearly by and the interface tracing was calculated as:

$$\partial\phi/\partial t + \nabla\cdot u\phi = 0, \tag{9}$$

The Semi-Implicit Method for Pressure Linked Equations-Consistent (SIMPLEC) pressure-velocity coupling method, PREssure STaggering Option (PRESTO) pressure discretization, momentum second-order upwind technique, volume fraction geometric reconstruction, and implicit temporal integration were employed. In the numerical algorithm, the magnetic volume force is added to the main code via a user function written in the C programming language (Fig. 2).

3- Results and Discussion

The mesh independence of the solution is evaluated with the droplet dimensionless volume. According to the results, 25,169 mesh cells are used for the simulations. The steady-state ferrofluid droplet formation process was performed by the volume of fluid method coupled with the magnetic field, velocity field, and interface tracking and validated with Liu et al. [2] with and without a magnetic field. After the validation, the effect of the magnetic field was analyzed as opposing velocities appear in the process. According to the results in Fig. 3 and Table 3, for Bm=0, The pressure drop, F_p, and the viscous drag force, F_μ, compress the ferrofluid tip pushing it downstream. The interfacial tension, F_σ, on the other hand, prevents the tip from moving forward. Since F_μ is proportional to the tip area and the velocity gradient. Therefore, the smaller

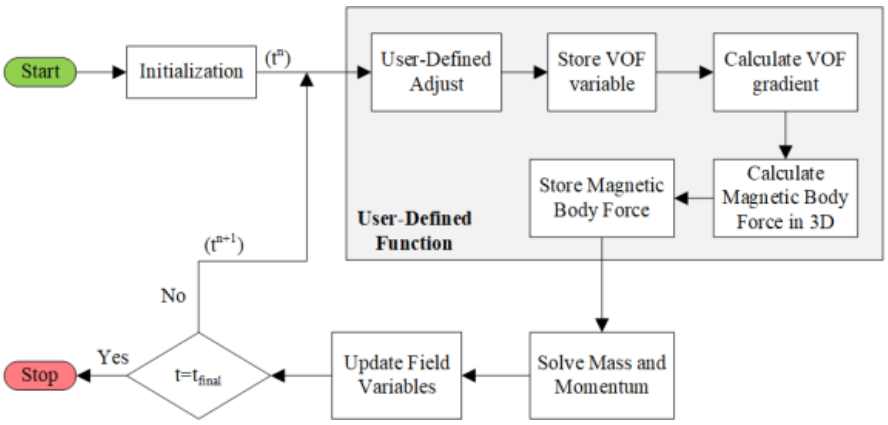

Fig. 2. Flowchart of the numerical solution.

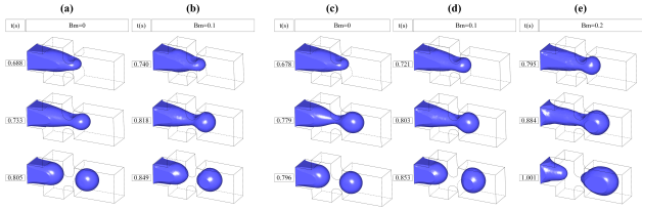

Fig. 3. Droplet formation process. a, b) Newtonian dispersed fluid for Bm=0,0.1. c, d, e) Carreau dispersed fluid for Bm=0,0.1,0.2.

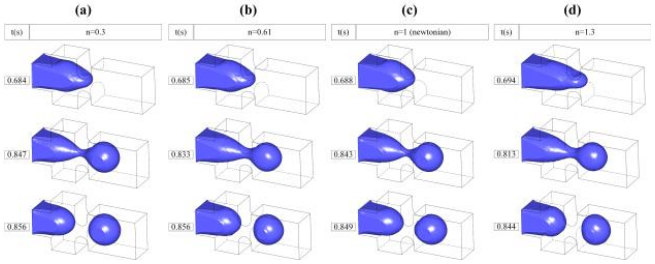

Fig. 4. Droplet formation process with the power-law fluid dispersed phase at Bm=0.1. a) n=0.3. b) n=0.61. c) n=1. d) n=1.3.

Table 2. dimensionless and separation times of the dispersed fluid models with/without the magnetic field.

	Newtonian Fluid		Carreau Fluid			Power-law Fluid		
						n=0.3	n=0.6	n=1.3
B_m	0	0.1	0	0.1	0.2		0.1	
V^*	0.655	0.781	0.651	0.839	1.561	0.836	0.729	0.697
t [s]	0.796	0.850	0.796	0.853	1.001	0.856	0.0856	0.844

droplet tip curvature at the beginning of the process leads to larger capillary forces, and higher pressure is required to move the tip through the connecting neck. The throat is then blocked as the dispersed phase progresses and the velocities inside the throat move up instead of downstream. Thus, Fp escalates dramatically outside the stream and the tip is pushed further. These interactions occur rapidly and finally, the high thread curvature reduces F_σ. Since the high F_p is present, the stretching of the ferrofluid from opposite directions continues until F_σ is no longer sufficient and the tip thread separates, forming a droplet.

When the uniform magnetic field is applied, the droplet formation involves an additional magnetic force, F_m, on the tip of the dispersed phase. The results show that all separations require more time. The thin thread is stretched more. Thus, it is longer and the tip is no longer spherical due to its lower interfacial tension. The pressure difference heightens gradually and larger elliptical droplets are formed with the same mechanism in a longer time. The Carreau dispersed fluid was explored next as in Fig. 3. For B_m=0 the droplets reached a similar volume in a shorter time while for B_m=0.1 larger volumes were achieved with less time. Since the stretching is more intense in higher magnetic fields, the almost double Bm created 86% growth in the droplet volume. Larger B_m, also reduces the pressure drop in addition to prolonging the time in which this pressure is reached.

The Power-law fluid was finally investigated for B_m=0.1 (Fig. 4). The results show that different n values have a rather similar separation time as the Carreau model. Thus, its influence on separation time is insignificant. As n is increased, the volume experiences change as the function given in Fig. 5

4- Conclusion

In this study, the external magnetic field's effect on the process of flow-focusing droplet formation has been studied numerically. Simulations have been performed for different values of the Bond number and three different Viscosity models. The droplet size, separation time, and pressure differences are compared. The results show that the flow is under F_μ, F_p, F_σ, and the additional Fm when the magnetic field is present. The magnetic force stretches the thread and lowers the pressure drop which results in the formation of larger droplets in longer times. The field affects the Carreau fluid more than the Newtonian fluid. For B_m=0.1, the Power-law model investigation also showed a volume reduction and enhancement for n<1.1 and n>1.1, respectively.

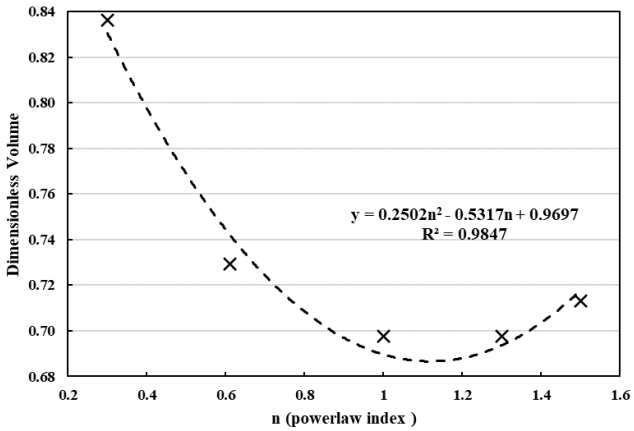

Fig. 5. The dimensionless volume of Power-law fluid droplet trend with changing n for Bm=0.1

References

[1] S.-H. Tan, N.-T. Nguyen, L. Yobas, T.G. Kang, Formation and manipulation of ferrofluid droplets at a microfluidicT-junction, Journal of Micromechanics and Microengineering, 20(4:045004) (2010) 1-10.

[2] J. Liu, Y.F. Yap, N.-T. Nguyen, Numerical study of the formation process of ferrofluid droplets, Physics of Fluids, 23(7:072008) (2011) 1-10.

[3] A. Taassob, M.K.D. Manshadi, A. Bordbar, R. Kamali, Monodisperse non-Newtonian micro-droplet generation in a co-flow device, Journal of the Brazilian Society of Mechanical Sciences and Engineering, 39(6) (2017) 2013-2021.

HOW TO CITE THIS ARTICLE

S. Mas-hafi, M. Esmaeili , Effect of Magnetic Field on Motion, Deformation, and Separation Time of Newtonian and Non-Newtonian Droplets in a Flow-Focusing Microchannel , Amirkabir J. Mech. Eng., 53(11) (2022) 1345-1348.

DOI: 10.22060/mej.2021.19257.6989